Polarization Symmetry Breaking and Pulse Train Generation from the Modulation of Light Waves

G. Millot, E. Seve, and S. Wabnitz
Laboratoire de Physique, Faculté des Sciences Mirande, Université de Bourgogne, Avenue A. Savary, B.P. 400, 21011 Dijon, France
(Received 17 January 1997)

The interplay of natural and self-induced birefringence leads to a nonlinear polarization symmetry breaking in the process of parametric four-photon scattering. The polarization instability was induced by mixing pump and probe light beams into an optical fiber, and the polarization dependent generation of ultrahigh repetition rate (200 GHz) solitonlike pulse trains was observed in the regime of normal group-velocity dispersion. [S0031-9007(97)03598-9]

PACS numbers: 42.65.Tg, 42.65.Re, 42.65.Sf, 42.81.Dp

Bifurcations of a potential function associated with a macroscopic physical system close to thermodynamic equilibrium lead to the emergence of new stable patterns or spatiotemporal structures [1]. The description of complex continuous systems in terms of a single potential entails a reduction of the dynamics to the interaction between a few degrees of freedom. Close to the instability threshold for a given mode, the other modes may be considered slaved to it. A well-known mechanism of pattern formation is the Benjamin-Feir modulational instability (MI) [2] of wave trains against a low-frequency perturbation. MI leads to the disintegration of wave trains in deep water [2], self-filamentation [3], or modulation [4] of Langmuir waves in plasmas [5] and light waves in optical dielectrics [6].

MI may be induced into an optical fiber by mixing two laser sources: in the anomalous dispersion regime, trains of solitons with THz repetition rates were generated more than ten years ago [7]. In the normal dispersion regime, MI may also be observed through cross-phase modulation between two copropagating pump waves of different color [8,9] or polarization [10,11]. Temporal instabilities and polarization symmetry breaking are also observed with counterpropagating optical beams [12]. In low-birefringence fibers, instability to low-frequency polarization modulations occurs only for beam powers above a certain threshold value. Taking the field intensity as an independent variable, polarization MI is a signature of a pitchfork bifurcation or second-order phase transition for the state of polarization of light in the nonlinear medium [13]. Indeed, previous experiments revealed a polarization asymmetric MI gain in optical fibers [14]. Nevertheless, the issue whether polarization MI might lead to solitonlike pulse train generation in the normal dispersion regime was not yet explored. In this work we observe a striking manifestation of light-activated polarization symmetry breaking. The experiments show, we believe for the first time, that induced polarization MI generates ultrahigh repetition rate trains of solitonlike pulses in the regime of normal dispersion of a nonlinear dispersive dielectric.

In the presence of a nonlinear polarization $\mathbf{P}_{\mathrm{NL}} = \chi[(\mathbf{E}\cdot\mathbf{E}^*)\mathbf{E} + (1/2)(\mathbf{E}\cdot\mathbf{E})\mathbf{E}^*]$ of third order in the electric field $\mathbf{E} = [\mathbf{x}u(z,t) + \mathbf{y}v(z,t)]f(x,y)\exp\{-i\omega t\}$ [$f(x,y)$ is a given transverse field profile], Maxwell's equations lead to two coupled nonlinear Schrödinger equations for the propagation of polarized light in optical fibers [10]. With dimensionless units and in a reference frame that rotates with the fiber's axes along the propagation direction at a rate of γ radians per unit length, one obtains

$$\begin{aligned} i\frac{\partial u}{\partial \xi} &= \beta\frac{\partial^2 u}{\partial \tau^2} + \frac{\Delta}{2}u + \frac{i\alpha}{2}v \\ &\quad - \left(|u|^2 + \frac{2}{3}|v|^2\right)u - \frac{1}{3}v^2u^*, \\ i\frac{\partial v}{\partial \xi} &= \beta\frac{\partial^2 v}{\partial \tau^2} - \frac{\Delta}{2}v - \frac{i\alpha}{2}u \\ &\quad - \left(|v|^2 + \frac{2}{3}|u|^2\right)v - \frac{1}{3}u^2v^*, \end{aligned} \tag{1}$$

for the two orthogonal polarization components u and v. Here $\beta = \pm 1/2$ for normal or anomalous group-velocity dispersion (GVD), respectively, Δ represents linear birefringence, and $\alpha = \gamma(2 - g)$, where $g \simeq 0.14$ is the twist-induced optical activity.

Consider first the twistless $\alpha = 0$ case for simplicity. Polarization modulational instability [11] may be described with the help of the projection $u(\xi,\tau) = A_0(\xi)$, $v(\xi,\tau) = \sqrt{2}A_1(\xi)\cos(\Omega\tau)$ from the infinite-dimensional system of partial differential equations (1) onto a single anharmonic oscillator equation for the spatial evolution of the complex amplitudes A_0 and A_1 [15]. One obtains

$$\frac{d\mathbf{S}}{d\xi} = [\mathbf{\Omega}_L + \mathbf{\Omega}_{\mathrm{NL}}(\mathbf{S})] \times \mathbf{S} \tag{2}$$

for the Stokes vector $\mathbf{S} \equiv (S_1, S_2, S_3)$ with components $S_1 = |A_0|^2 - |A_1|^2$, $S_2 = A_0^*A_1 + \text{c.c.}$, and $S_3 = iA_0^*A_1 + \text{c.c.}$, whereas $\mathbf{\Omega}_L = (\mu, 0, 0)$ and $\mathbf{\Omega}_{\mathrm{NL}} = [(3S_0 - 7S_1), -4S_2, 4S_3]/12$, with $\mu \equiv \beta\Omega^2 + \Delta$. The invariants $S_0 = |A_0|^2 + |A_1|^2$ and $\Gamma = 7S_1^2 + 4S_2^2 - 4S_3^2 - 6(4\mu + 1)S_1$ permit us to reduce Eq. (2) to the one-dimensional

motion of an equivalent particle in a potential well. A symmetry-breaking bifurcation of the pump beam [i.e., the eigenmode $S_1 = S_0, S_2 = S_3 = 0$ of Eq. (2)] leads to an unstable saddle point in the potential whenever $0 < \mu(\Delta, \Omega)/S_0 < 2/3$. The signature of this instability is the exponential growth (with a spatial rate, or gain, G) of optical intensity into the side modes of frequency detunings Ω within a certain range. The expression for μ shows that, in the normal dispersion regime, a pump beam may be modulationally unstable with either $\Delta < 0$ (slow mode) or $\Delta > 0$ (fast mode). In the last case, the pump power P_0 must be larger than a threshold value $P_t \equiv 3\Delta/2R$, where $R = 2\pi n_2/\lambda_p A_{\text{eff}}$, λ_p is the pump wavelength, n_2 is the nonlinear refractive index, and $A_{\text{eff}} = [\int |f|^2\, dx\, dy]^2 / \int |f|^4\, dx\, dy$ is the effective area of the fiber mode. In fact, linearization of Eq. (2) in the plane tangent to the pump eigenmode leads to the MI intensity gain $G = 2[\mu(2S_0/3 - \mu)]^{1/2}$.

Figure 1 illustrates the frequency dependence of G in real units, for the experimental conditions described below, and the pump power $P = 112$ W. Here the solid and dashed curves are obtained for a pump aligned with the slow or the fast axis of the birefringent fiber, respectively. As can be seen, the polarization symmetry breaking leads to nonoverlapping, strongly asymmetric gain profiles.

The experimental apparatus for observing the induced modulational polarization instabilities is shown in Fig. 2. Quasi-cw operation was achieved by using nanosecond pulses. The pump beam was delivered by a cw tunable ring dye laser, subsequently amplified by a three-stage dye cell. The dye amplifier was in turn pumped by a frequency-doubled, injection-seeded and Q-switched Nd:YAG laser (at the wavelength $\lambda = 532.26$ nm), operating at a repetition rate of 25 Hz. The signal was obtained by frequency shifting an intense beam (1 MW peak power) from the Nd:YAG laser. The frequency shift resulted from the self-stimulated Raman effect taking place in a gas sample. The gas was carbone dioxide at a pressure of 1.7×10^5 Pa, and the first Stokes wave, shifted by 1388 cm^{-1} (41.64 THz, ν_1 band) from the input laser, was filtered with a direct vision prism (DVP). The power threshold for Raman scattering was reduced by using a multiple-pass cell (MPC) with 25 passes. The 4 ns pump beam pulses were sent into an optical delay line (ODL) for their synchronization with the 2 ns signal pulses. Orthogonally polarized pump and signal of adjustable power were obtained through a half-wave plate and two Glan laser polarizers (P) followed by a set of neutral-density filters (F). In the experiment, the pump wavelength was tuned around $\lambda_p = 575$ nm, whereas the signal was fixed at $\lambda_s = 574.746$ nm. Pump and signal beams were combined by a beam splitter (BS) and focused with a 40× microscope objective (MO) in 6.8 m of ultralow birefringence spun fiber, with a cutoff wavelength of 470 nm and a nominal linear retardance of less than 1°. The relatively short length of fiber used in the experiment led to negligible pump depletion owing to stimulated Raman scattering. The fiber dispersion at λ_p coincides with the fused silica value $k'' = 0.06$ ps^2 m^{-1}. A weak linear fiber birefringence was introduced by winding the fiber onto a spool with a diameter $d = 2R = 14.5$ cm: this induces a linear birefringence $\delta n = \lambda_p/L_b = 0.133(r/R)^2 \simeq 10^{-7}$, where $r = 62.5$ μm is the fiber cladding radius and $L_b = 5.8$ m is the resulting beat length. The fiber effective area $A_{\text{eff}} = 1.5 \times 10^{-11}$ m^2 was determined from the measurement of the far-field distribution. By combining these data with the silica value of the nonlinear refractive index $n_2 = 3.2 \times 10^{-20}$ m^2 W^{-1}, one obtains a threshold power $P_t = 70$ W for the MI of the fast fiber mode. We inserted a half-wave plate in front of the MO for the control of the orientation of the two orthogonal input beams with respect to the fiber birefringence axes. At the fiber output, the beam was collimated and split into two parts. A first part

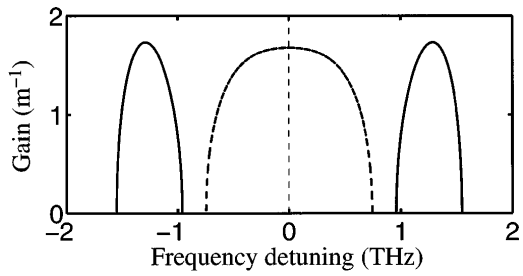

FIG. 1. Modulational instability gain vs frequency detuning of sidebands from the pump: solid (dashed) curve for slow (fast) axis excitation.

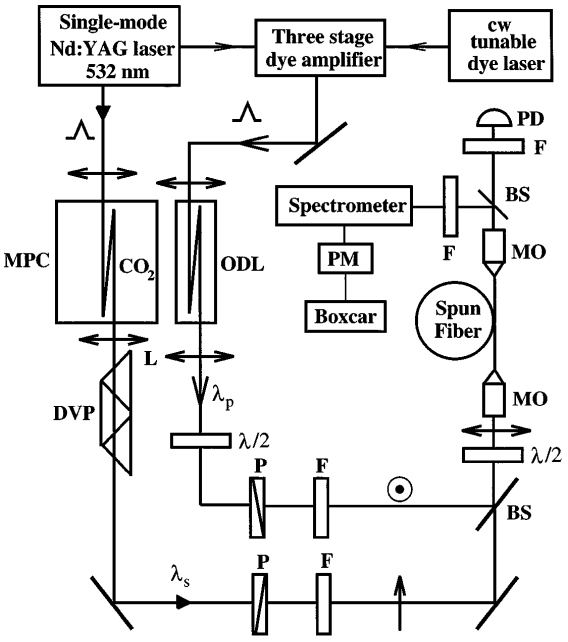

FIG. 2. Schematic diagram of the experimental apparatus.

was used to measure the peak power of each laser beam, whereas the second part was sent into a 50 cm spectrometer with a resolution of better than 0.04 nm. The optical signal was recorded by a photomultiplier and then sampled and averaged by a boxcar integrator.

The orientation of the fiber axes was determined by the following procedure [16]. The power of the orthogonal pump and signal (with a given frequency detuning of, say, 0.3 THz) was fixed, and their orientation with respect to the fiber axes was controlled by rotating the half-wave plate at the fiber input. The optical intensity of the generated idler at the wavelength λ_i was then measured. Figure 3(a) shows the variation of the idler intensity for a full turn of the pump polarization. The pump and signal peak powers were equal to 112 and 1.1 W, respectively. Since the slow fiber mode was stable under the above input conditions, its direction may be identified with the absolute minimum of idler intensity. On the other hand, Fig.3(b) confirms that the position of the fast axis may also be obtained [besides from a simple 90° rotation away from the slow axis as determined from Fig. 3(a)] from the minima of the generated idler intensity with a signal detuning increased up to 1.2 THz. In the absence of fiber axes twisting, the generated idler intensity has a mirror symmetry with respect to the axes positions. The asymmetric polarization dependence of the gain in Fig. 3(a) indicates the presence of a moderate amount of twist.

For a quantitative evaluation of the twist contribution to the linear fiber birefringence, we numerically calculated the polarization dependence of the MI gain directly by linearizing Eqs. (1) about the pump. In fact, for an arbitrary orientation of the pump polarization with respect to the birefringence axes, upper and lower sidebands have nonvanishing components on both axes. By applying the Floquet method to the resulting spatially varying (owing to pump nonlinear polarization rotation) linearized system of equations for the four sidebands one obtains the effective MI gain $G = 2\ln(|\Lambda|)/L$ over the fiber length L. Here Λ is the largest modulus eigenvalue of the principal solution matrix associated with the linearized sideband equations. A comparison between this computation (taking into account the averaging of the gain G over the intensity profile of the pulsed pump and signal) and the results of Fig. 3 show a good qualitative agreement. The only fitting parameter in the computation was the twist rate: one obtains a small twist of 0.08 rad/m.

The determination of the fiber axes directions permitted a clear observation of polarization symmetry breaking as predicted by the theory (see Fig. 1). To this end, we aligned the polarization of the pump with either the slow or the fast fiber axis, and we scanned the spectral intensity of the waves emerging from the fiber. Figure 4 shows measured output light spectra with a signal frequency detuning of 1.2 THz, and a pump (of power $P = 112$ W) parallel to either the fast [Fig. 4(a)] or the slow [Fig. 4(b)] axis. As can be seen, in agreement with the predictions of Fig. 1, the stability of the fast fiber mode prevents a transfer of photons from the pump into the signal and the idler. On the other hand, for slow mode pumping the signal falls into the MI gain bandwidth: as a result, a deep polarization modulation of the pump wave is observed. We observed that, for slow axis pumping, the output sidebands remain essentially orthogonally polarized to the pump on the slow mode, which justifies *a posteriori* the validity of the ansatz that leads to Eq. (2). Moreover,

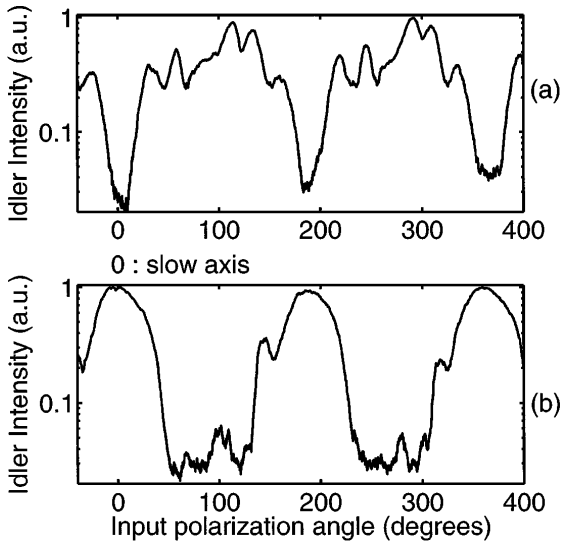

FIG. 3. Intensity (logarithmic scale) of the generated idler vs pump angle, for a pump power of 112 W and signal detuning of (a) 0.3 and (b) 1.2 THz.

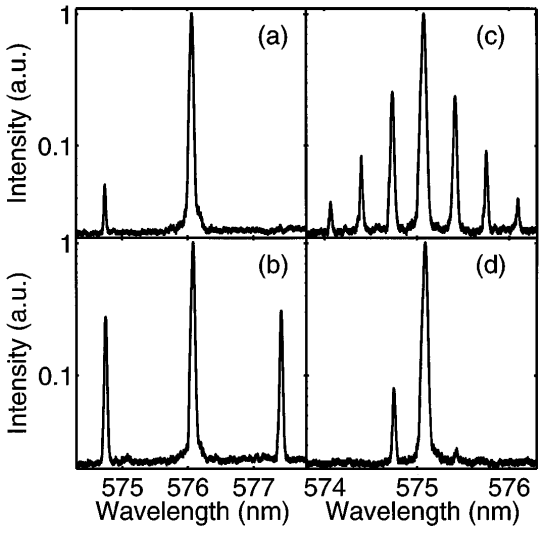

FIG. 4. Output spectral intensities (logarithmic scale) with the pump polarized along either the fast axis (a) or the slow axis (b). The pump power is 112 W and probe frequency detuning is 1.2 THz. (c),(d) As in (a),(b), with a probe detuning of 0.3 THz.

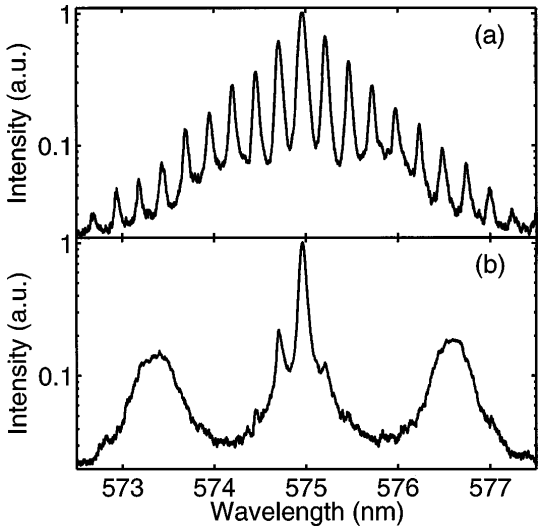

FIG. 5. As in Fig. 4, with a pump power of 268 W and the probe detuning of 0.23 THz.

no higher-order sidebands are produced, owing to the relatively narrow width of the parametric of MI gain curve (see Fig. 1).

Figures 4(c)–4(d) show that the portrait of the instability is drastically altered if the signal frequency detuning from the pump is reduced down to 0.3 THz. In fact, in this case (see Fig. 1) the slow mode is stable whereas the fast mode is unstable, which leads to the strong nonlinear development of polarization modulations in Fig. 4(c). As can be seen, the modulated waves capture a large fraction of the pump energy. Figure 1 also shows that both the first and the second harmonic of the initial modulation fall within the relatively flat MI gain bandwidth, which enhances the conversion into a cascade of higher-order sidebands. The polarization state of these modulated waves no longer remains orthogonal to the pump, which indicates that the nonlinear dynamics of the multimode wave mixing with fast mode excitation may be properly described by higher-order finite-dimensional mode truncations. Finally, Fig. 4(d) confirms that the slow mode is stable with respect to the injected signal.

The MI-induced breakup of an intense beam into a train of ultrashort solitary wave pulses is well displayed by the results of Fig. 5(a), where the pump power on the fast axis was increased up to 268 W, and the signal power was 1.9 W. Basic Fourier transform considerations indicate that the nearly triangular (in a logarithmic scale) envelope of the comb associated with the spectral intensity of the pulse train involves wave-front durations of the order of 400 fs. Figure 5(b) shows that a rotation of the pump polarization by 90° leads to spontaneous (i.e., noise-induced) MI, along with significant pump spectral broadening owing to self-phase modulation. In the present experiments, the ratio of pump to signal power was kept in the range of 100–140. For smaller pump to signal power ratios, the large-signal theory of four-wave mixing in birefringent fibers predicts strong deviations of the effective MI gain from the linearized stability analysis values [17]: experimental studies of this effect will be reported elsewhere.

In conclusion, these observations provide a clear evidence of light-activated polarization symmetry breaking in the propagation of modulated waves in a nonlinear birefringent dielectric. By inducing polarization MI, we could generate high-repetition rate (0.2–0.3 THz) subpicosecond pulse trains in a normally dispersive nonlinear medium.

[1] G. Nicolis and I. Prigogine, *Self-Organization in Nonequilibrium Systems, from Dissipative Structures to Order through Fluctuations* (Wiley, New York, 1977).
[2] T. J. Benjamin and J. E. Feir, J. Fluid Mech. **27**, 417 (1967).
[3] V. I. Bespalov and V. I. Talanov, Pis'ma Zh. Eksp. Teor. Fiz. **3**, 471 (1966) [JETP Lett. **3**, 307 (1966).
[4] V. I. Karpman and E. M. Krushkal, Zh. Eksp. Teor. Fiz. **55**, 530 (1968) [Sov. Phys. JETP **28**, 277 (1969)].
[5] Yu. Ya. Brodskii, A. G. Litvak, S. I. Neuchuev, and Ya. Z. Slutsker, Pis'ma Zh. Eksp. Teor. Fiz. **45**, 176 (1987) [JETP Lett. **45**, 217 (1987)].
[6] K. Tai, A. Hasegawa, and A. Tomita, Phys. Rev. Lett. **56**, 135 (1986).
[7] K. Tai, A. Tomita, J. L. Jewell, and A. Hasegawa, Appl. Phys. Lett. **49**, 236 (1986).
[8] G. P. Agrawal, *Nonlinear Fiber Optics* (Academic, New York, 1995), 2nd ed., Chap. 7, and references therein.
[9] MI may also be observed with pump and probe in opposite dispersion regimes: G. P. Agrawal, P. L. Baldeck, and R. R. Alfano, Phys. Rev. A **40**, 5063 (1989).
[10] A. L. Berkhoer and V. E. Zakharov, Zh. Eksp. Teor. Fiz. **58**, 903 (1970) [Sov. Phys. JETP **31**, 486 (1970)].
[11] S. Wabnitz, Phys. Rev. A **38**, 2018 (1988).
[12] A. L. Gaeta, R. W. Boyd, J. A. Ackerhalt, and P. W. Milonni, Phys. Rev. Lett. **58**, 2432 (1987).
[13] B. Daino, G. Gregori, and S. Wabnitz, J. Appl. Phys. **58**, 4512 (1985); H. G. Winful, Opt. Lett. **11**, 33 (1986).
[14] S. F. Feldman, D. A. Weinberger, and H. G. Winful, Opt. Lett. **15**, 311 (1990); J. Opt. Soc. Am. B **10**, 1191 (1993); S. G. Murdoch, R. Leonhardt, and J. D. Harvey, Opt. Lett. **20**, 866 (1995).
[15] S. Trillo and S. Wabnitz, Phys. Lett. A **159**, 252 (1991).
[16] In very low-birefringence fibers, the birefringence axes do not coincide, in general, with the two orthogonal linear polarizations that emerge linearly polarized.
[17] G. Cappellini and S. Trillo, Opt. Lett. **16**, 895 (1991).